Matrilin-1 Is an Inhibitor of Neovascularization*

Matthew J. Foradori[‡§], **Qian Chen**[¶], **Cecilia A. Fernandez**[‡§], **Jay Harper**[‡§], **Xin Li**[¶], **Paul C. W. Tsang**[∥], **Robert Langer**[**], **and Marsha A. Moses**[‡§1]

*From the ‡Program in Vascular Biology and Department of Surgery, Boston Children's Hospital, Boston, Massachusetts 02115 and §Harvard Medical School, Boston, Massachusetts 02115, the ¶Department of Orthopaedics, Warren Alpert Medical School of Brown University/Rhode Island Hospital, Providence, Rhode Island 02903, the ∥Department of Molecular, Cellular, and Biomedical Sciences, University of New Hampshire, Durham, New Hampshire 03824, and the **Department of Biochemical Engineering, Massachusetts Institute of Technology, Cambridge, Massachusetts 02139*

Background: The relative avascularity of cartilage has made it a promising source of angiogenesis inhibitors.
Results: MATN-1, identified by mass spectrometry, suppresses capillary endothelial cell proliferation and migration.
Conclusion: MATN-1 is a novel inhibitor of neovascularization *in vivo* and *in vitro*.
Significance: This is the first demonstration that MATN-1 is an inhibitor of both normal and pathological neovascularization.

In the course of conducting a series of studies whose goal was to discover novel endogenous angiogenesis inhibitors, we have purified matrilin-1 (MATN-1) and have demonstrated, for the first time, that it inhibits neovascularization both *in vitro* and *in vivo*. Proteins were extracted from cartilage using a 2 M NaCl, 0.01 M HEPES buffer at 4 °C, followed by concentration of the extract. The concentrate was fractionated by size exclusion chromatography, and fractions were then screened for their ability to inhibit capillary endothelial cell (EC) proliferation *in vitro*. Fractions containing EC inhibitory activity were pooled and further purified by cation exchange chromatography. The resulting fractions from this step were then screened to isolate the antiangiogenic activity *in vitro*. This activity was identified by tandem mass spectrometry as being MATN-1. Human MATN-1 was cloned and expressed in *Pichia pastoris* and purified to homogeneity. Purified recombinant MATN-1, along with purified native protein, was shown to inhibit angiogenesis *in vivo* using the chick chorioallantoic membrane assay by the inhibition of capillary EC proliferation and migration. Finally, using a MATN-1-deficient mouse, we showed that angiogenesis during fracture healing was significantly higher in MATN-1$^{-/-}$ mice compared with the wild type mice as demonstrated by *in vivo* imaging and by elevated expression of angiogenesis markers including PECAM1, VEGFR, and VE-cadherin.

Cartilage is an avascular and relatively tumor-resistant tissue that is composed predominantly of proteoglycans, several types of collagen, and noncollagenous matrix proteins (1–3). The resistance of cartilage to capillary invasion has long been pos-

tulated to be a function of the presence of endogenous inhibitors of angiogenesis, which inhibit new blood vessel formation from pre-existing vessels. The first of these inhibitors purified to homogeneity was a cartilage-derived tissue inhibitor of metalloproteinases (TIMP),[2] a protein that was demonstrated to be a potent inhibitor of capillary EC proliferation and migration *in vitro*, and angiogenesis *in vivo* in both the chick chorioallantoic membrane (CAM) assay and the corneal pocket assay (4, 5). Shortly thereafter, a chondrocyte-derived angiogenesis inhibitor, a 35.5-kDa protein isolated from chondrocyte primary cultures, was shown to inhibit angiogenesis *in vitro* in EC proliferation and migration assays and *in vivo* in the CAM assay (6). Chondromodulin-I, a 25-kDa protein isolated from bovine epiphyseal cartilage was shown to inhibit capillary tube formation in *in vitro* (7–9) and tenomodulin, another protein that shares homology with chondromodulin-I, was shown to inhibit angiogenesis *in vitro* as well (9–12). Troponin I, a 23-kDa contractile protein typically found in muscle, was isolated from bovine cartilage, and demonstrated to inhibit EC proliferation *in vitro*, angiogenesis in the CAM and mouse corneal pocket assays *in vivo*, as well as tumor metastasis *in vivo* (13).

Nonmammalian cartilage has also been studied as a potential source of angiogenesis inhibitors. Lee and Langer were the first to demonstrate that an extract of shark cartilage could significantly inhibit tumor neovascularization (14). Since then, several laboratories have isolated partially purified fractions from this type of cartilage which have been shown to inhibit at least one of the processes associated with angiogenesis. For example, U995, a fraction containing 10- and 14-kDa peptides isolated from the blue shark, *Prionace glauca*, interfered with human umbilical vein endothelial cell proliferation and migration (15). SCF2, a glycosaminoglycan whose principal component is keratan sulfate, is a 10-kDa proteoglycan that has been reported to inhibit EC proliferation *in vitro*, as well as tumor-induced angiogenesis in the cornea of rabbits and angiogenesis in CAM

² The abbreviations used are: TIMP, tissue inhibitor of metalloproteinases; bFGF, basic fibroblast growth factor; Bis-Tris, bis(2-hydroxyethyl)iminotris(hydroxymethyl)methane; CAM, chorioallantoic membrane; FMT, fluorescence molecular tomography; MATN-1, matrilin-1.

assays *in vivo* (1). SCAIF80, an 80-kDa protein isolated from shark cartilage, has been shown to significantly suppress EC proliferation and migration in a dose-dependent matter *in vitro* (16), and SCP1, a 13.7-kDa protein with sequence similarities to parvalbumin, was reported to inhibit angiogenesis in the rat aortic ring assay (17). AE-941, an "angiogenic mixture" (18) isolated from *Squalus acanthias* cartilage, has been shown to inhibit angiogenesis *in vitro* in the rat aortic ring vessel assay (19) and *in vivo* in the CAM assay (20). In addition, the shark tissue inhibitor of metalloproteinase 3 (sTIMP-3), has been cloned and characterized from the cloudy dogfish, *Scyliorhinus torazame* (21). It was later shown to inhibit migration and tube formation in bovine aortic endothelial cells (22).

In this study, we have purified and identified a novel inhibitor of angiogenesis, matrilin-1 (MATN-1). Having demonstrated its ability to inhibit angiogenesis *in vivo*, we determined that MATN-1 exerted this suppression of neovascularization by inhibiting angiogenesis growth factor-driven capillary endothelial cell proliferation and migration. These studies were supported by both *in vitro* gain-of-function studies and *in vivo* loss-of-function experiments using MATN-1 KO mice. MATN-1, formerly known as cartilage matrix protein, is an abundant component of cartilage (23). A modular protein, MATN-1 mediates interactions between a variety of matrix components (24) and, as a structural protein, it binds to biglycan and decorin (25), collagen (26), cartilage oligomeric matrix protein (27), as well as to itself (28). To our knowledge, this report is the first to document the ability of this structural protein to suppress new capillary growth *in vivo* and suggests that its targeting may be of potential clinical significance.

EXPERIMENTAL PROCEDURES

Extract Preparation—The chondrocranium cartilage of the spiny dogfish (*S. acanthias*) was harvested and scraped free of muscle and connective tissue as described previously (4, 14). The prepared cartilage (250 g) was homogenized and extracted in 4 liters of a 2 M NaCl, 0.01 M HEPES, 3 mM EDTA, 0.02% NaN$_3$ extraction buffer for 4 days under constant agitation, utilizing a modification of a previous procedure (4). The extraction solution was filtered with gauze, centrifuged at 6500 × *g* for 2 h to remove particulates, then concentrated using a Vivacell 250 (Sartorius Stedim Biotech) to a final volume of ~5 ml. The concentrated cartilage extract had a final protein concentration of 7.8 mg/ml. All procedures were performed at 4 °C.

Purification and Identification of MATN-1—A 40-mg sample of concentrated cartilage extract, dialyzed against Bio-Gel A-1.5m buffer (4 M guanidine HCl, 20 mM Tris, pH 7.6) (Bio-Rad 151-0450, per manufacturer's instructions) overnight, was applied to a Bio-Gel A-1.5m Sepharose size exclusion column (5 × 50) at a flow rate of 1.0 ml/min; fractions were collected every 5 min. Fractions were screened for their ability to inhibit both EC proliferation and matrix metalloproteinase (MMP) activity (Fig. 1*A*). Given that cartilage had already been reported to contain an antiangiogenic activity that was identified as being an MMP inhibitor (4), fractions were screened for both of these activities to identify a novel inhibitor of neovascularization. Fractions 22–34 from the column were enriched in the ability to inhibit EC proliferation and were pooled, dialyzed

overnight to remove the guanidine HCl, and then applied to a Bio-Rex 70 column (Bio-Rad) and fractionated, as previously described by us (4). Fractions 2 and 5 (Fig. 1*B*), which contained the antiproliferative activity, were pooled and dialyzed to remove excess salts, then subjected to electrophoresis on 12% SDS-polyacrylamide gels (Bio-Rad) or 12% Bis-Tris NU-PAGE gels (Invitrogen) run under denaturing conditions followed by visualization by either silver or SYPRO Ruby (Invitrogen) staining (29). Protein bands were excised from the gel, subjected to tryptic digestion, and analyzed by MALDI-TOF mass spectrometry (Perceptive STR, Applied Biosystems) to determine the molecular masses of the proteins and for peptide mapping of the tryptic digests using a 337-nm wavelength laser for desorption and the reflectron mode of analysis. Using the MSFit and SEQUEST (30) search programs, the peptide maps generated were searched against a FASTA database of public domain proteins constructed of protein entries in the nonredundant database held by the NCBI and Swiss Protein Database. Peptide matches identified by MSFit were filtered according to their MOWSE (molecular mass search) score, percentage of masses matched, molecular mass, and number of observations of peptides and proteins.

Cloning, Expression, and Purification of MATN-1—The cMATN-1 gene was cloned using a pcDNA3.1 vector with cMATN-1 insert (31) and primers specific for the mature form of chick MATN-1. The human MATN-1 (hMATN-1) gene was cloned from normal adult human lung and trachea first strand cDNA (Biochain Institute, Inc., Hayward, CA). For the cloning of both the chick and human MATN-1 into the pPICZαC expression plasmid, the cDNAs for MATN-1 were amplified by PCR using two primers that covered the translation start codon (primer 1) and the stop codon (primer 2) of cartilage matrix protein cDNA, respectively. The two primers were designed in such a way that primer 1 contained a XhoI site and primer 2 contained a polyhistidine tag (to aid in purification) and a XbaI site (for hMATN-1, primer 1, 5′-CCGCTCGAGATGAGGGT-CCTCTCTGGCA-3′; primer 2, 5′-GCTCTAGATCAATGA-TGATGATGATGATGTTAGACAACTGTGTTC-3′; for cMATN-1, primer 1, 5′-CCGCTCGAGAAAAGACCTCCTC-AGCCCAGAGG-3′; primer 2, 5′-GCTCTAGATCAATGAT-GATGATGATGATGGATGATCTTATTCTC-3′). The full-length MATN-1 PCR products were subcloned into pCR4-TOPO vector (Invitrogen). After confirmation of the sequence, the MATN-1 genes were ligated into the yeast expression vector pPICZαC (Invitrogen). Linearized vectors (PmeI) were electroporated into the yeast *Pichia pastoris* for expression (Invitrogen), and integrants were selected by culturing on YPDS (2% peptone, 1% yeast extract, 2% glucose, 1 M sorbitol, 2% agar) plates with 100 μg/ml zeocin (Invitrogen) for 3 days. Successful insertion of chick and human genes of interest into the *Pichia* genome were verified by PCR using *Pichia*-specific primers, which also verified that recombination occurred at the correct site. Expression of the gene of interest is under the control of the methanol-inducible AOX1 promoter.

Five *Pichia* clones each of cMATN-1 and hMATN-1 were tested for their expression levels and the clones from each set expressing the highest amount of protein were chosen for subsequent studies. The expression conditions were as follows:
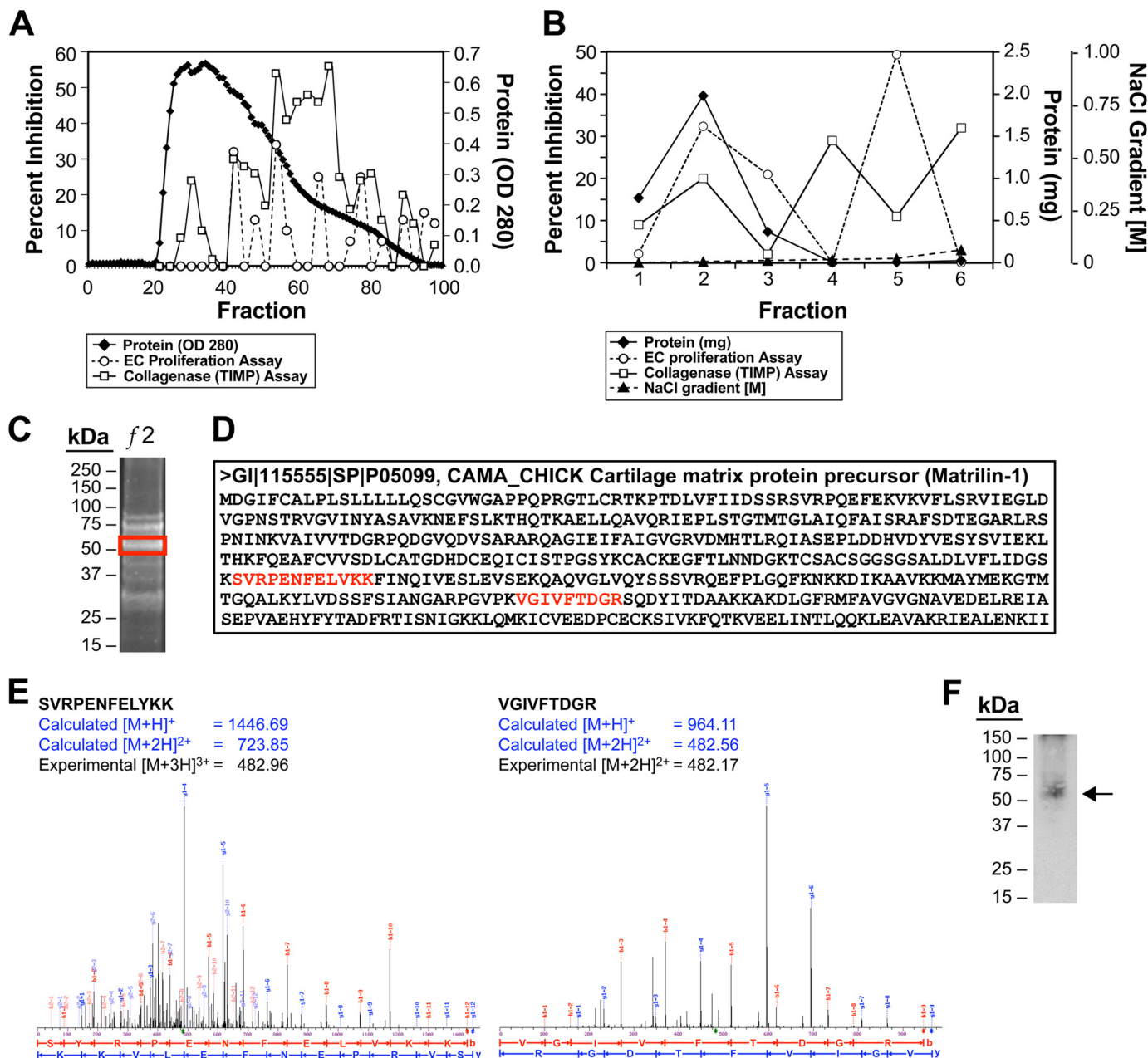
FIGURE 1. **Purification of anti-angiogenic activity in concentrated cartilage extract and identification of antiangiogenic activity as being MATN-1.** *A*, fractions 22–34 of concentrated cartilage extract fractionated on Bio-Gel A-1.5m size exclusion chromatography significantly inhibited mitogen-stimulated capillary EC proliferation. Fractions 52–75 contained metalloproteinase-inhibiting activity but had no significant effect on EC proliferation. *B*, fractions 22–34 were pooled, concentrated, dialyzed, and subjected to further purification on a Bio-Rex 70 cation exchange column. Fractions 2 and 5 contained inhibitory activity of FGF-stimulated capillary EC proliferation with no significant TIMP activity. *C*, the antiproliferative activity from the Bio-Rex 70 column was concentrated and electrophoresed on a 12% SDS-polyacrylamide gel followed by staining with SYPRO Ruby. *C–E*, bands were excised from the gel and analyzed by mass spectrometry with the band highlighted by the *red box* having two peptide matches identifying it as being matrilin-1. *F*, to confirm this identification, a sample of the same fraction from the cation exchange column was electrophoresed on a 12% SDS-polyacrylamide gel and probed with an antibody to matrilin-1.

25-ml overnight cultures were grown at 30 °C in yeast extract peptone dextrose medium (YPD, 1% yeast extract, 2% peptone, 2% dextrose) containing 100 μg/ml zeocin. Cell pellets were collected after 24 h by centrifugation at 1500 × *g*. Cultures were induced to express the recombinant proteins by resuspending the cell pellets in 250 ml of buffered methanol-complex medium (BMMY, 2% peptone, 1% yeast extract, 100 mM potassium phosphate, pH 6.0, 1.34% yeast nitrogenous base, 1% methanol) and allowed to grow for 24 h at 30 °C with constant

shaking. Medium containing the secreted expressed protein was cleared of cell content by centrifugation at 5000 × *g*.

Purification of Recombinant MATN-1—Expressed recombinant chicken and human MATN-1 proteins were initially purified from the yeast media using histidine affinity binding to a nickel-nitrilotriacetic acid-agarose resin (Qiagen) under native conditions. Expressed protein in 800 ml of pooled, cleared medium was allowed to bind to 5 ml of resin in a prepacked column by gravity flow at 4 °C. The resin was washed with 50 ml

(10 volumes) of buffer containing 10 mM imidazole (50 mM NaH_2PO_4, 300 mM NaCl, 10 mM imidazole, pH 8.0) to reduce nonspecific binding. Protein was then eluted using 25 ml (5 volumes) of elution buffer containing 100 mM imidazole (50 mM NaH_2PO_4, 300 mM NaCl, 100 mM imidazole, pH 8.0) and concentrated by centrifugation using membrane concentrators with 10-kDa molecular mass cutoff (Centriprep, Amicon, Beverly, MA). Purity was confirmed by silver staining of SDS-polyacrylamide gels and tandem mass spectrometry.

Cell Culture—Capillary ECs, isolated from bovine adrenal cortex, were a kind gift from Dr. Judah Folkman and Catherine Butterfield (Boston Children's Hospital). Cells were maintained in Dulbecco's modified Eagle's medium (DMEM; Invitrogen) containing 10% calf serum (HyClone) and 3 ng/ml basic fibroblast growth factor (bFGF) in 10% CO_2 at 37 °C, as previously reported (4).

Endothelial Cell Proliferation Assay—Capillary EC proliferation was measured as reported previously (4, 6, 13). Briefly, capillary ECs were plated on pregelatinized 96-well plates at a density of 2000 cells/well in DMEM supplemented with 5% calf serum and allowed to attach for 24 h. The next day, cells were treated with fresh medium with or without 1 ng/ml bFGF and challenged with the test proteins at various concentrations. All samples were tested in duplicate. Control wells contained cell treated with medium alone or medium with bFGF. After 72 h, the medium was removed, and the cells were lysed in buffer containing Triton X-100 and the phosphatase substrate *p*-nitrophenyl phosphate. After a 2-h incubation at 37 °C, NaOH was added to each well to terminate the reaction, and cell density was determined by colorimetric analysis using a Spectra-Max 190 multiwell plate reader (Molecular Devices). All samples were tested in duplicate in at least three independent experiments.

Capillary Endothelial Cell Migration—Capillary EC migration was studied using a modified Boyden chamber as previously described (4, 32). The upper half of Transwell (8-μm pore; Costar) membranes were coated with fibronectin (10 μg/ml; BD Biosciences) overnight at 4 °C to facilitate cell adhesion. Coated membranes were rinsed with PBS and allowed to air dry immediately before use. Cells were detached by trypsinization and resuspended at a final concentration of 0.5×10^6 cells/ml in serum-free DMEM containing 0.1% BSA. Cells were added to the upper chamber of the Transwell and allowed to migrate toward the bottom chamber containing DMEM, or DMEM supplemented with the chemoattractant bFGF for 4 h in a humidified incubator containing 5% CO_2. Transwell filters were rinsed once with PBS and fixed and stained using a Diff-Quik kit (Baxter) following the manufacturer's protocol. Stained filters were cut out of the chamber and mounted onto slides using Permount (Sigma). The number of migrated cells were counted (three fields from each membrane were captured using a 10× objective), and images were captured with a CCD camera using SPOT software. Total migration/membrane was quantified from the captured images using Scion Image software (National Institutes of Health). All experiments were run in triplicate.

MMP Inhibitory Activity—MMP inhibitory activity was assessed using a quantitative $[C^{14}]$collagen film assay, as described previously (4, 32). An IC_{50} unit was defined as the amount of protein necessary to inhibit the proteolytic activity of collagenase by 50%.

Angiogenesis Inhibitory Activity in Vivo—The CAM assay was conducted as reported previously (4, 32). Three-day-old chick embryos were removed from their shells and incubated in plastic Petri dishes for 3 days. On embryonic day 6, samples and controls were mixed into methylcellulose and allowed to dry. The discs were applied to the surfaces of developing CAMs, above the dense subectodermal plexus. After an incubation of 48 h, the eggs were examined for vascular reactions under a dissecting scope and photographed. All samples were tested in triplicate for each treatment.

Mice Tibia Fracture Model—Animals were studied at Coro Center Facilities of Rhode Island Hospital. National Institutes of Health guidelines for the care and use of animals were observed, and the study was approved by Rhode Island Hospital IACUC. Six- to 8-week-old male mice were used in the experiments. MATN-1$^{-/-}$ ($n = 5$) mice and WT mice ($n = 5$) of the same genetic background (C57BL/6J) were genotyped using PCR. The animals were used to create fracture models as described previously (1, 33). In brief, animals were anesthetized by intraperitoneal injection of a ketamine (Bioniche Pharma) and medetomidine (Orion Corporation, Espoo, Finland) mixture (75 $\pm$1 mg/kg). The animals were prepared for surgery by shaving and scrubbing of both hind limbs. A longitudinal short incision was made at the knee, and a 0.5-mm hole was drilled above the tibial tuberosity. A 30-gauge stainless-steel needle (Hamilton, Reno, NV) was introduced into the intramedullary canal of the tibia. The wound was closed, and the procedure was repeated on the contralateral side. A closed transverse mid-diaphyseal tibia fracture was created by three-point bending in the right tibia, and the animal was allowed to move freely after recovery from anesthesia with the intraperitoneal injection of Antisedan (1 mg/kg) (Orion Corporation). A preoperative cefadroxil (25 mg/kg) was administered subcutaneously to prevent infection. Buprenex (Reckitt Benckiser Healthcare, UK; 0.03 mg/kg) was given once preoperatively and two times per day during the first 3 days after surgery to relieve pain.

Fluorescence Molecular Tomography Measurements of Angiogenesis—The commercially available fluorescent probes, AngioSense™ (FRFP750, excitation 750t10 nm; emission 780t10 nm) (VisEn Medical Inc., Woburn, MA) was used in this study. The AngioSense 750 is a fluorescent *in vivo* blood pool imaging agent that enables imaging of blood vessels and angiogenesis. The adult mouse dose of 2 nmol in 150 ml of saline (13.3 mM) or ~80 nmol/kg body weight was utilized. The probes were delivered to the animals by intraperitoneal injection 24 h before taking the images with the Fluorescence Molecular Tomography (FMT) system (VisEn Medical Inc., Woburn, MA) on day 4 after surgery. Twenty-four hours after the probe injection, mice were anesthetized with a solution of ketamine and medetomidine and imaged using the VisEn FMT system, as described previously (34). Three-dimensional regions of interest were drawn around the tibial fracture limbs and control limbs, and a threshold was applied equal to 10% of the maximum value of fluorescence in each reconstructed volume. The peak concentration (in nmol/liter) and total amount (in pmol) of fluoro-

chrome were automatically calculated relative to internal standards generated with known concentrations of appropriate dyes.

Callus mRNA Expression—The RNeasy Fibrous Tissue Mini kit (74704, Qiagen) was used to extract RNA from the fracture calluses 14 days after surgery with the following modification. After the mice were sacrificed, the fracture calluses were placed in RNA later (Qiagen) and stored at −80 °C until RNA extraction. The calluses were ground into a fine powder using mortar and pestle with liquid nitrogen and extracted according to the instructions provided with the kit. Quality and quantity of RNA were determined using a Nano-drop (Ambion, Austin, TX). mRNA was determined by real-time quantitative reverse-transcriptase PCR (RT-PCR). Total RNA (1 μg) was transcribed into cDNA using iScripTM (Bio-Rad) with 40 ng/μl of the resulting cDNA used as the template to quantify the relative content of mRNA by RT-PCR using Sso Fast EvaGreen Supermix (Bio-Rad) with CFX 96 Real Time PCR system (Bio-Rad). To normalize the data, mRNA expression of a housekeeping gene, *18S*, was also determined. The cycle threshold (Ct) values for *18S* RNA and that of samples were measured and calculated by Excel (Office 2007, Microsoft, Redmond, WA). Relative transcript levels were calculated as $x = 2^{-\Delta\Delta Ct}$, in which $\Delta\Delta Ct = \Delta E - \Delta C$, and $\Delta E = Ct_{exp} - Ct_{18s}$; $\Delta C = Ct_{ctl} - Ct_{18s}$.

RESULTS

Identification of Matrilin-1—The band migrating at ~52 kDa consistent with the molecular mass of MATN-1 was excised from the gel (Fig. 1C) and subjected to mass spectrometry analysis as described above. The MOWSE score reported by MSFit was 547 with 6 matching peptides (40% coverage); the protein was identified as cartilage matrix protein precursor or matrilin-1 (*Gallus gallus* EMBL-EBI accession number 115555). SEQUEST also identified the protein as matrilin-1 (*G. gallus* accession number P05099) with a reported Xcor value of 3.04 or higher for four peptides; again, the protein was identified as a cartilage matrix protein precursor (matrilin-1; P05099) (Fig. 1, C–E). Immunoblot analysis using a monoclonal antibody to MATN-1 (1:3000) confirmed the identification of the 52-kDa protein band as being MATN-1. This antibody was a gift from Dr. Paul Goetinck (35) (Fig. 1F).

MATN-1 Inhibits Angiogenesis in the Chick CAM Assay— The chick CAM assay was used to determine whether MATN-1 could suppress angiogenesis *in vivo*. We observed significant inhibition of embryonic neovascularization in this assay as evidenced by the avascular zone elicited by representative CAM treatment with 10 μg (350 nM) of recombinant chicken MATN-1 or 5 μg recombinant human MATN-1 (Fig. 2).

MATN-1 Inhibits Endothelial Cell Proliferation and Migration—Given its ability to inhibit angiogenesis *in vivo*, we next asked how MATN-1 might be exerting this antiangiogenic effect. We tested MATN-1 in two different assay systems, which measured the inhibition of angiogenic mitogen-driven capillary endothelial cell proliferation and migration, two processes essential for successful angiogenesis. Purified native chick MATN-1 (Fig. 3A), recombinant chick MATN-1 (Fig. 3B), and recombinant human MATN-1 (Fig. 3C) all suppressed EC proliferation. The IC$_{50}$ for each of the three treatments was
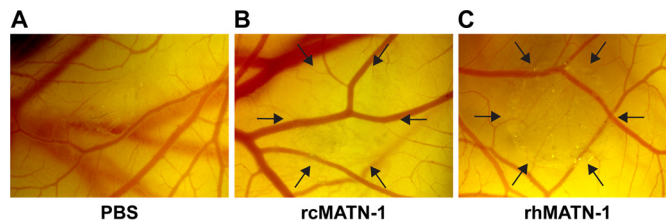

A **B** **C**

PBS **rcMATN-1** **rhMATN-1**

FIGURE 2. **MATN-1 suppresses angiogenesis *in vivo*.** Recombinant chick MATN-1 and human MATN-1 inhibit angiogenesis *in vivo* as indicated by the avascular zones localizing the zones of new capillary inhibition on the chick chorioallantoic membrane induced by 10 μg of rcMATN-1 (*B*) and 5 μg of rhMATN-1 (*C*), *versus* a lack of inhibition in the representative control (*A*).
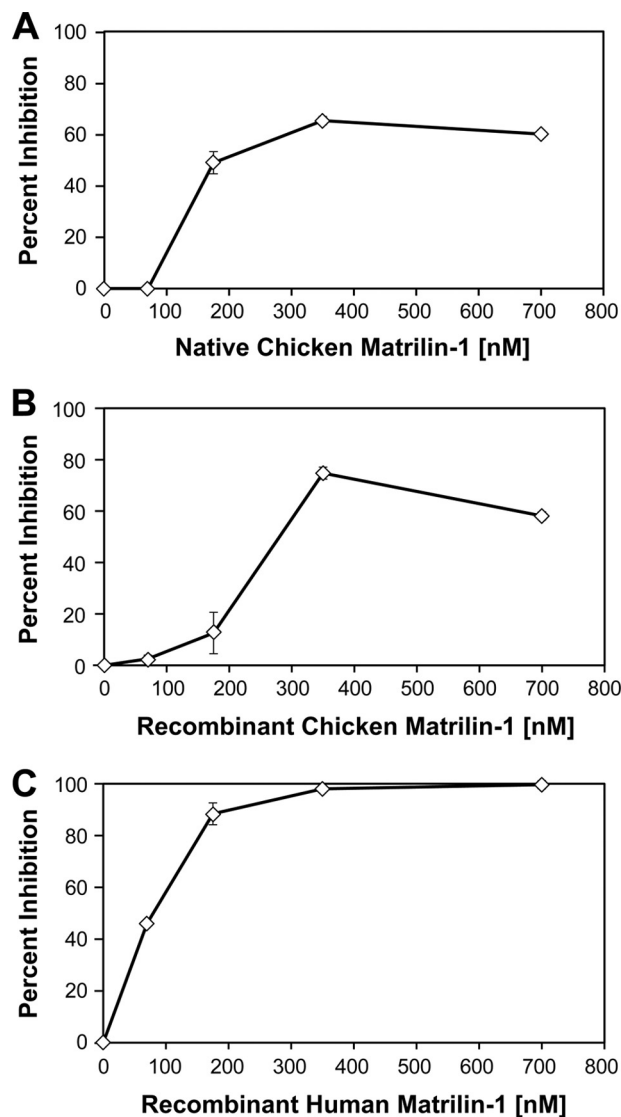

FIGURE 3. **Inhibition of bFGF-stimulated bovine capillary endothelial cell growth by MATN-1.** Purified cMATN-1 (*A*), rcMATN-1 (*B*), and rhMATN-1 (*C*) were tested for their ability to inhibit bFGF-stimulated EC growth. In all cases, MATN-1 was found to inhibit EC proliferation in dose-dependent manner.

~175 nM, 275 nM, and 75 nM, respectively. When purified native chick MATN-1, recombinant chick MATN-1, or recombinant human MATN-1 (Fig. 4) was tested for its effect on EC in a Transwell migration assay, we found that migration was inhibited in a dose-dependent manner with an IC$_{50}$ of ~75 nM, 80 nM, and 10 nM, respectively.
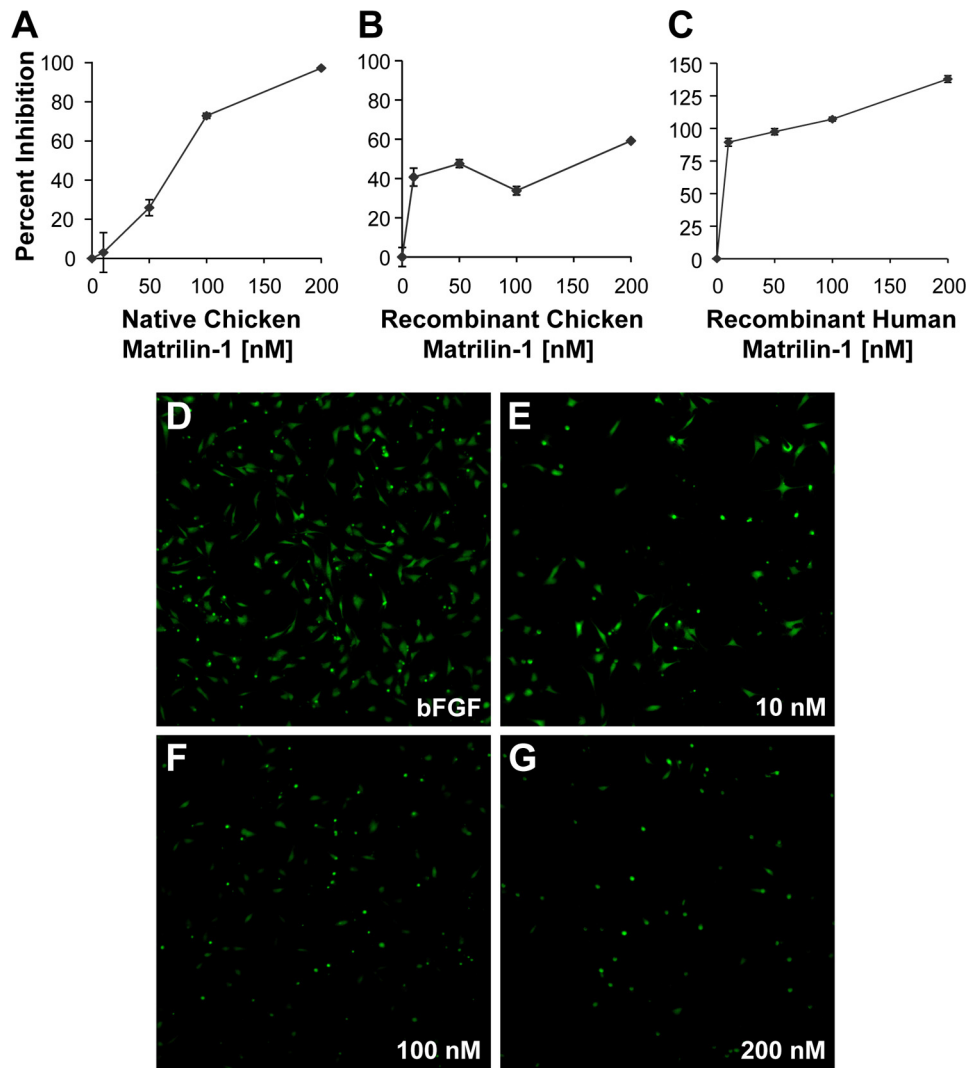
FIGURE 4. **Inhibition of bFGF-stimulated bovine capillary EC migration by MATN-1.** *A–C*, purified cMATN-1 (*A*), rcMATN-1 (*B*), and rhMATN-1 (*C*) were tested for their ability to inhibit bFGF-stimulated EC migration. In all cases, MATN-1 was found to inhibit EC migration in a dose-dependent manner. Cells were labeled as described under "Experimental Procedures" and allowed to migrate through the Transwell. *D–G*, representative images show migrated cells treated with 0 nM (*D*), 10 nM (*E*), 100 nM (*F*), and 200 nM (*G*) recombinant human MATN-1.

MATN-1$^{-/-}$ Mice Induce Angiogenesis in the Early Period of Fracture Healing—We next complemented these *in vitro* gain-of-function studies by conducting *in vivo* loss-of-function experiments using MATN-1 KO mice. The FMT images and tomographic reconstructions showing angiogenesis in the injured site (Fig. 5) provide a clear visualization and quantification of neovascularization in the fracture site and control limb. Fig. 5 shows a three-dimensional rendering of the vasculature in WT and MATN-1$^{-/-}$ mice, respectively, injected with AngioSense 24 h before FMT analysis taken on day 4 after fracture. The fractured tibia of MATN-1$^{-/-}$ mice displayed a significant AngioSense signal, which was 1.76-fold higher than that of the WT mice ($p = 0.0041$). There was no significant difference between MATN-1$^{-/-}$ and WT mice in the control tibia ($p = 0.0970$). MATN-1$^{-/-}$ mice had a 1.87-fold higher AngioSense signal compared with WT mice ($p = 0.0156$). These findings from the FMT analysis indicated that there was significantly more vascularization at the early stage of fracture healing in MATN-1$^{-/-}$ mice.

To confirm these findings, we analyzed the expression of angiogenesis-related gene markers. The animals were sacrificed on day 14 after fracture, and total RNA was isolated from the fracture calluses for RT-PCR analysis. The mRNA expression of angiogenesis-relevant factors, including PECAM1, VEGFR, and VE-cadherin were examined by RT-PCR (Fig. 6). The results demonstrated that, 14 days after fracture, MATN-1$^{-/-}$ mouse calluses expressed significantly higher PECAM1 ($p = 0.0041$), VEGFR ($p = 0.0115$), and VE-cadherin ($p = 0.0004$) expression levels compared with those of WT mice. Taken together, these results demonstrate that MATN-1 inhibits angiogenesis in the early phase of fracture healing.

DISCUSSION

In the present study, we demonstrate for the first time that MATN-1 is an inhibitor of angiogenesis. We have further demonstrated that the mechanism by which MATN-1 inhibits angiogenesis is through the potent inhibition of growth factor-stimulated capillary endothelial cell proliferation and migra-
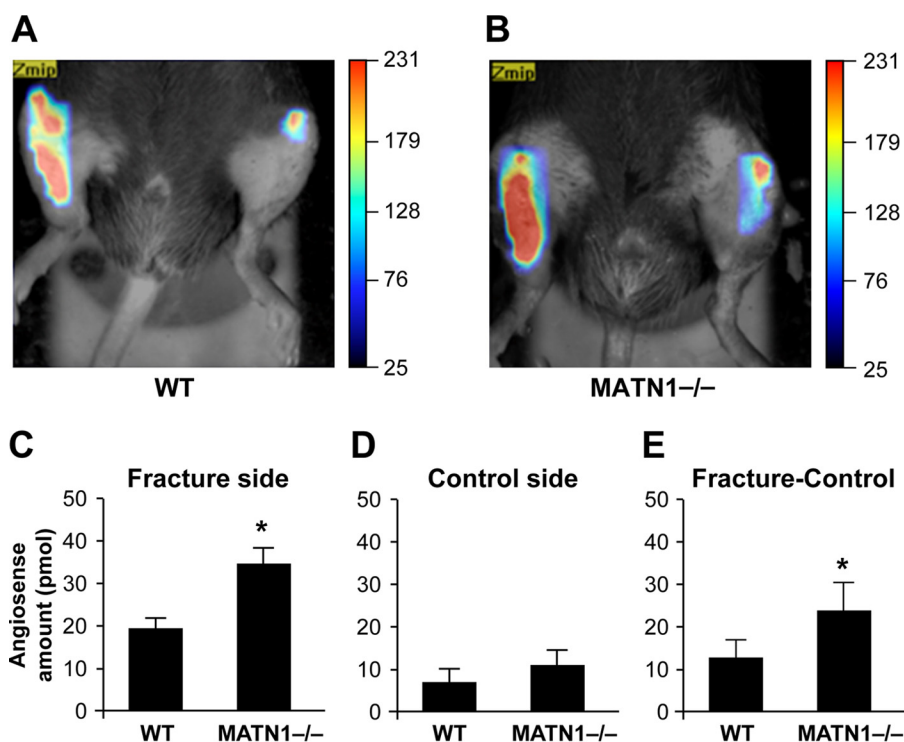
FIGURE 5. ***In vivo* imaging and quantification of AngioSense signal in WT and MATN-1 KO mice on day 4 after fracture.** *A* and *B*, representative volume renderings were taken at the same color gating from WT (*A*) and MATN-1$^{-/-}$ mice (*B*) injected with AngioSense according to the manufacturer's directions. *C–E*, the total amount of fluorescence (pmol) was quantified in specific regions of interest encompassing fracture tibias and control tibias. MATN-1 KO mice showed a significant 1.76-fold increase in AngioSense signal ($p = 0.0041$) in fractured tibia compared with WT mice (*C*). There was no difference between MATN-1 KO and WT mice in control tibias (*D*; $p = 0.0970$). MATN-1 KO mice had 1.87-fold higher AngioSense signal compared with WT mice (*E*), when the signal amount of fractured tibia was subtracted from that of control tibias ($p = 0.0156$).*, $p < 0.05$; $n = 5$. *Error bars*, S.E.
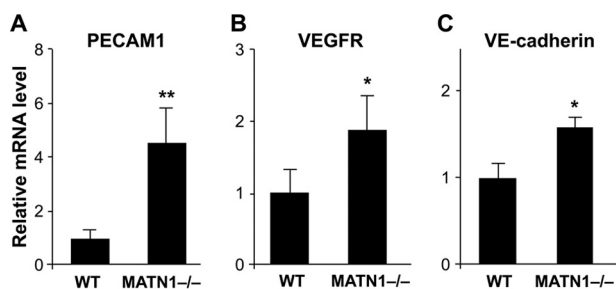

FIGURE 6. **mRNA expression of angiogenesis-related genes in the fracture calluses of MATN-1 KO and WT mice on day 14 determined by real-time RT-PCR analysis.** MATN-1 KO mice had significantly higher PECAM1 ($p = 0.0041$) (*A*), VEGFR ($p = 0.0115$) (*B*), and VE-cadherin ($p = 0.0004$) (*C*) expression levels compared with WT mice. *, $p < 0.05$, $n = 5$. *Error bars*, S.E.

tion. These two activities have been shown by our laboratory and many others to be necessary mechanisms for the formation of new capillaries from pre-existing vessels, *i.e.* angiogenesis (36). These *in vivo* data are supported by both the *in vitro* gain-of-function experiments (Figs. 3 and 4) and an *in vivo* loss-of-function study using MATN-1 KO mice (Figs. 5 and 6).This novel activity of MATN-1 may be due to structural and/or regulatory roles of MATN-1 in cartilage. MATN-1 contains the von Willebrand factor type A domain, also called the I domain in the integrin family, which is responsible for the MATN-1 interaction with the extracellular matrix and integrins via the metal ion-dependent adhesion sites (MIDAS) motif (28). This interaction may affect angiogenesis which critically depends on cell-matrix interaction (4, 36). This hypothesis remains to be tested in future.

MATN-1 is a modular matrix protein capable of mediating interactions between a variety of matrix components through von Willebrand factor type A domains that intervene through adhesion via MIDAS. These domains exhibit high affinity toward collagen which also possesses von Willebrand factor type A-like domains (24), as well as biglycan and decorin (25). The discovery of a noncollagenous matrix protein as an angiogenesis inhibitor is not unprecedented. Decorin, a small proteoglycan composed of a protein core and a covalently linked side chain of chrondroitin/dermatan sulfate, has been shown to inhibit endothelial cell migration, attachment, and the formation of endothelial tube-like structures (37, 38). MATN-1 is the newest member of the family of matrix-derived inhibitors of neovascularization. As is the case with thrombospondin-1 and -2 (39–41), it distinguishes itself from other inhibitors in this family such as endostatin (42, 43), tumstatin (44, 45), arresten (46), and canstatin (47) in that these latter inhibitors are proteolytically processed products of larger, largely angiogenesis-inert matrix proteins (48, 49).

Our group and others have reported the discovery of novel cartilage-derived antiangiogenic proteins (4, 6, 13), and a number of other groups have reported the presence of potential inhibitors of neovascularization from nonmammalian sources of cartilage as well. For example, fractionated samples of shark cartilage extracts, such as U-995 (15), SCF2 (1), SCAIF80 (16), and DCAI (50), have shown preliminary promise in inhibiting angiogenesis; however, the active biomolecule has yet to be purified and identified. SCP1, a low molecular mass protein extracted from shark cartilage, with a sequence similar to

α-parvalbumin, a calcium-binding molecule, has been shown to exert some antiangiogenic activity in a rat aortic ring assay (17). Neovastat, a purified fraction of shark cartilage extract with MMP inhibitory activity (51), was developed for clinical use and demonstrated limited success in early phase I/II clinical trials as treatment for non-small cell lung cancer and renal cell carcinoma (52–54). Ultimately, in phase III trials, when coupled with standard chemotherapy, Neovastat had no additive effect on the improvement of overall survival in patients with unresectable stage III non-small cell lung cancer (55). Neovastat has had limited success in the treatment of renal cell carcinoma (56).

MATN-1 is an inhibitor of both capillary endothelial cell proliferation and migration, processes that, when driven by endothelial cell mitogens, represent critical processes required to assess angiogenic potential. It is an inhibitor of angiogenesis *in vivo* in a model of normal, embryonic angiogenesis such as the CAM, as well as in a model of pathological neovascularization and in the mice tibia fracture model. As such, this protein, either alone or in combination with other inhibitors, may be useful in the treatment of a number of diseases that are characterized by dysregulated neovascularization.

REFERENCES

1. Liang, J. H., and Wong, K. P. (2000) The characterization of angiogenesis inhibitor from shark cartilage. *Adv. Exp. Med. Biol.* **476,** 209–223
2. Kim, D. H., Kim, Y. T., Cho, J. J., Bae, J. H., Hur, S. B., Hwang, I., and Choi, T. J. (2002) Stable integration and functional expression of flounder growth hormone gene in transformed microalga, *Chlorella ellipsoidea*. *Mar. Biotechnol.* **4,** 63–73
3. Hiraki, Y., and Shukunami, C. (2005) Angiogenesis inhibitors localized in hypovascular mesenchymal tissues: chondromodulin-I and tenomodulin. *Connect. Tissue Res.* **46,** 3–11
4. Moses, M. A., Sudhalter, J., and Langer, R. (1990) Identification of an inhibitor of neovascularization from cartilage. *Science* **248,** 1408–1410
5. Langer, R., and Moses, M. A. (1991) Angiogenesis inhibitors. *Biotechnology* **9,** 630–634
6. Moses, M. A., Sudhalter, J., and Langer, R. (1992) Isolation and characterization of an inhibitor of neovascularization from scapular chondrocytes. *J. Cell Biol.* **119,** 475–482
7. Hiraki, Y., Inoue, H., Iyama, K., Kamizono, A., Ochiai, M., Shukunami, C., Iijima, S., Suzuki, F., and Kondo, J. (1997) Identification of chondromodulin I as a novel endothelial cell growth inhibitor: purification and its localization in the avascular zone of epiphyseal cartilage. *J. Biol. Chem.* **272,** 32419–32426
8. Kusafuka, K., Hiraki, Y., Shukunami, C., Kayano, T., and Takemura, T. (2002) Cartilage-specific matrix protein, chondromodulin-I (ChM-I), is a strong angio-inhibitor in endochondral ossification of human neonatal vertebral tissues *in vivo*: relationship with angiogenic factors in the cartilage. *Acta Histochem.* **104,** 167–175
9. Shukunami, C., and Hiraki, Y. (2007) Chondromodulin-I and tenomodulin: the negative control of angiogenesis in connective tissue. *Curr. Pharm. Des.* **13,** 2101–2112
10. Shukunami, C., Oshima, Y., and Hiraki, Y. (2001) Molecular cloning of tenomodulin, a novel chondromodulin-I related gene. *Biochem. Biophys. Res. Commun.* **280,** 1323–1327
11. Oshima, Y., Sato, K., Tashiro, F., Miyazaki, J., Nishida, K., Hiraki, Y., Tano, Y., and Shukunami, C. (2004) Anti-angiogenic action of the C-terminal domain of tenomodulin that shares homology with chondromodulin-I. *J. Cell Sci.* **117,** 2731–2744
12. Shukunami, C., Oshima, Y., and Hiraki, Y. (2005) Chondromodulin-I and tenomodulin: a new class of tissue-specific angiogenesis inhibitors found in hypovascular connective tissues. *Biochem. Biophys. Res. Commun.* **333,** 299–307
13. Moses, M. A., Wiederschain, D., Wu, I., Fernandez, C. A., Ghazizadeh, V., Lane, W. S., Flynn, E., Sytkowski, A., Tao, T., and Langer, R. (1999) Troponin I is present in human cartilage and inhibits angiogenesis. *Proc. Natl. Acad. Sci. U.S.A.* **96,** 2645–2650
14. Lee, A., and Langer, R. (1983) Shark cartilage contains inhibitors of tumor angiogenesis. *Science* **221,** 1185–1187
15. Sheu, J. R., Fu, C. C., Tsai, M. L., and Chung, W. J. (1998) Effect of U-995, a potent shark cartilage-derived angiogenesis inhibitor, on anti-angiogenesis and anti-tumor activities. *Anticancer Res.* **18,** 4435–4441
16. Shen, X. R., Ji, D. M., Hu, Y. Q., Jia, F. X., Wang, L., Chu, Z. Y., and Ren, D. M. (2001) SCAIF80, a novel inhibitor of angiogenesis, and its effect on tumor growth. *Sheng Wu Hua Xue Yu Sheng Wu Wu Li Xue Bao* **33,** 99–104
17. Rabbani-Chadegani, A., Abdossamadi, S., Bargahi, A., and Yousef-Masboogh, M. (2008) Identification of low-molecular-weight protein (SCP1) from shark cartilage with anti-angiogenesis activity and sequence similarity to parvalbumin. *J. Pharm. Biomed. Anal.* **46,** 563–567
18. Gingras, D., Renaud, A., Mousseau, N., Beaulieu, E., Kachra, Z., and Béliveau, R. (2001) Matrix proteinase inhibition by AE-941, a multifunctional antiangiogenic compound. *Anticancer Res.* **21,** 145–155
19. Béliveau, R., Gingras, D., Kruger, E. A., Lamy, S., Sirois, P., Simard, B., Sirois, M. G., Tranqui, L., Baffert, F., Beaulieu, E., Dimitriadou, V., Pépin, M. C., Courjal, F., Ricard, I., Poyet, P., Falardeau, P., Figg, W. D., and Dupont, E. (2002) The antiangiogenic agent Neovastat (AE-941) inhibits vascular endothelial growth factor-mediated biological effects. *Clin. Cancer Res.* **8,** 1242–1250
20. Dupont, E., Falardeau, P., Mousa, S. A., Dimitriadou, V., Pepin, M. C., Wang, T., and Alaoui-Jamali, M. A. (2002) Antiangiogenic and antimetastatic properties of Neovastat (AE-941), an orally active extract derived from cartilage tissue. *Clin. Exp. Metastasis* **19,** 145–153
21. Kim, J. T., Kim, M. S., Bae, M. K., Song, H. S., Ahn, M. Y., Kim, Y. J., Lee, S. J., and Kim, K. W. (2001) Cloning and characterization of tissue inhibitor of metalloproteinase-3 (TIMP-3) from shark, *Scyliorhinus torazame*. *Biochim. Biophys. Acta* **1517,** 311–315
22. Kang, J. A., Kim, J. T., Song, H. S., Bae, M. K., Yi, E. Y., Kim, K. W., and Kim, Y. J. (2003) Anti-angiogenic and anti-tumor invasive activities of tissue inhibitor of metalloproteinase-3 from shark, *Scyliorhinus torazame*. *Biochim. Biophys. Acta* **1620,** 59–64
23. Paulsson, M., and Heinegård, D. (1982) Radioimmunoassay of the 148-kilodalton cartilage protein: distribution of the protein among bovine tissues. *Biochem. J.* **207,** 207–213
24. Neame, P. J., Tapp, H., and Azizan, A. (1999) Noncollagenous, nonproteoglycan macromolecules of cartilage. *Cell. Mol. Life Sci.* **55,** 1327–1340
25. Wiberg, C., Klatt, A. R., Wagener, R., Paulsson, M., Bateman, J. F., Heinegård, D., and Mörgelin, M. (2003) Complexes of matrilin-1 and biglycan or decorin connect collagen VI microfibrils to both collagen II and aggrecan. *J. Biol. Chem.* **278,** 37698–37704
26. Winterbottom, N., Tondravi, M. M., Harrington, T. L., Klier, F. G., Vertel, B. M., and Goetinck, P. F. (1992) Cartilage matrix protein is a component of the collagen fibril of cartilage. *Dev. Dyn.* **193,** 266–276
27. Mann, H. H., Ozbek, S., Engel, J., Paulsson, M., and Wagener, R. (2004) Interactions between the cartilage oligomeric matrix protein and matrilins: implications for matrix assembly and the pathogenesis of chondrodysplasias. *J. Biol. Chem.* **279,** 25294–25298
28. Chen, Q., Zhang, Y., Johnson, D. M., and Goetinck, P. F. (1999) Assembly of a novel cartilage matrix protein filamentous network: molecular basis of differential requirement of von Willebrand factor A domains. *Mol. Biol. Cell* **10,** 2149–2162
29. Roy, R., Louis, G., Loughlin, K. R., Wiederschain, D., Kilroy, S. M., Lamb, C. C., Zurakowski, D., and Moses, M. A. (2008) Tumor-specific urinary matrix metalloproteinase fingerprinting: identification of high molecular weight urinary matrix metalloproteinase species. *Clin. Cancer Res.* **14,** 6610–6617
30. MacCoss, M. J., Wu, C. C., and Yates, J. R., 3rd (2002) Probability-based validation of protein identifications using a modified SEQUEST algorithm. *Anal. Chem.* **74,** 5593–5599
31. Zhang, Y., and Chen, Q. (2000) Changes of matrilin forms during endochondral ossification: molecular basis of oligomeric assembly. *J. Biol.*

Chem. **275,** 32628–32634

32. Fernández, C. A., Butterfield, C., Jackson, G., and Moses, M. A. (2003) Structural and functional uncoupling of the enzymatic and angiogenic inhibitory activities of tissue inhibitor of metalloproteinase-2 (TIMP-2): loop 6 is a novel angiogenesis inhibitor. *J. Biol. Chem.* **278,** 40989–40995

33. Hiltunen, A., Vuorio, E., and Aro, H. T. (1993) A standardized experimental fracture in the mouse tibia. *J. Orthop. Res.* **11,** 305–312

34. Zilberman, Y., Kallai, I., Gafni, Y., Pelled, G., Kossodo, S., Yared, W., and Gazit, D. (2008) Fluorescence molecular tomography enables *in vivo* visualization and quantification of nonunion fracture repair induced by genetically engineered mesenchymal stem cells. *J. Orthop. Res.* **26,** 522–530

35. Chen, Q., Johnson, D. M., Haudenschild, D. R., and Goetinck, P. F. (1995) Progression and recapitulation of the chondrocyte differentiation program: cartilage matrix protein is a marker for cartilage maturation. *Dev. Biol.* **172,** 293–306

36. Harper, J., and Moses, M. A. (2006) Molecular regulation of tumor angiogenesis: mechanisms and therapeutic implications. *EXS* **96,** 223–268

37. de Lange Davies, C., Engesaeter, B. Ø., Haug, I., Ormberg, I. W., Halgunset, J., and Brekken, C. (2001) Uptake of IgG in osteosarcoma correlates inversely with interstitial fluid pressure, but not with interstitial constituents. *Br. J. Cancer* **85,** 1968–1977

38. Grant, D. S., Yenisey, C., Rose, R. W., Tootell, M., Santra, M., and Iozzo, R. V. (2002) Decorin suppresses tumor cell-mediated angiogenesis. *Oncogene* **21,** 4765–4777

39. Bornstein, P. (2009) Thrombospondins function as regulators of angiogenesis. *J. Cell Commun. Signal.* **3,** 189–200

40. Good, D. J., Polverini, P. J., Rastinejad, F., Le Beau, M. M., Lemons, R. S., Frazier, W. A., and Bouck, N. P. (1990) A tumor suppressor-dependent inhibitor of angiogenesis is immunologically and functionally indistinguishable from a fragment of thrombospondin. *Proc. Natl. Acad. Sci. U.S.A.* **87,** 6624–6628

41. Ren, B., Yee, K. O., Lawler, J., and Khosravi-Far, R. (2006) Regulation of tumor angiogenesis by thrombospondin-1. *Biochim. Biophys. Acta* **1765,** 178–188

42. O'Reilly, M. S., Boehm, T., Shing, Y., Fukai, N., Vasios, G., Lane, W. S., Flynn, E., Birkhead, J. R., Olsen, B. R., and Folkman, J. (1997) Endostatin: an endogenous inhibitor of angiogenesis and tumor growth. *Cell* **88,** 277–285

43. Wen, W., Moses, M. A., Wiederschain, D., Arbiser, J. L., and Folkman, J. (1999) The generation of endostatin is mediated by elastase. *Cancer Res.* **59,** 6052–6056

44. Petitclerc, E., Boutaud, A., Prestayko, A., Xu, J., Sado, Y., Ninomiya, Y., Sarras, M. P., Jr., Hudson, B. G., and Brooks, P. C. (2000) New functions for non-collagenous domains of human collagen type IV: novel integrin ligands inhibiting angiogenesis and tumor growth *in vivo*. *J. Biol. Chem.* **275,** 8051–8061

45. Maeshima, Y., Colorado, P. C., Torre, A., Holthaus, K. A., Grunkemeyer, J. A., Ericksen, M. B., Hopfer, H., Xiao, Y., Stillman, I. E., and Kalluri, R. (2000) Distinct antitumor properties of a type IV collagen domain derived from basement membrane. *J. Biol. Chem.* **275,** 21340–21348

46. Nyberg, P., Xie, L., Sugimoto, H., Colorado, P., Sund, M., Holthaus, K., Sudhakar, A., Salo, T., and Kalluri, R. (2008) Characterization of the anti-angiogenic properties of arresten, an $\alpha 1 \beta 1$ integrin-dependent collagen-derived tumor suppressor. *Exp. Cell Res.* **314,** 3292–3305

47. Kamphaus, G. D., Colorado, P. C., Panka, D. J., Hopfer, H., Ramchandran, R., Torre, A., Maeshima, Y., Mier, J. W., Sukhatme, V. P., and Kalluri, R. (2000) Canstatin, a novel matrix-derived inhibitor of angiogenesis and tumor growth. *J. Biol. Chem.* **275,** 1209–1215

48. Sottile, J. (2004) Regulation of angiogenesis by extracellular matrix. *Biochim. Biophys. Acta* **1654,** 13–22

49. Sund, M., Nyberg, P., and Eikesdal, H. P. (2010) Endogenous matrix-derived inhibitors of angiogenesis. *Pharmaceuticals* **3,** 3021–3039

50. Luo, H., Xu, J., and Yu, X. (2007) Isolation and bioactivity of an angiogenesis inhibitor extracted from the cartilage of *Dasyatis akajei*. *Asia Pac. J. Clin. Nutr.* **16,** 286–289

51. Falardeau, P., Champagne, P., Poyet, P., Hariton, C., and Dupont, E. (2001) Neovastat, a naturally occurring multifunctional antiangiogenic drug, in phase III clinical trials. *Semin. Oncol.* **28,** 620–625

52. Batist, G., Patenaude, F., Champagne, P., Croteau, D., Levinton, C., Hariton, C., Escudier, B., and Dupont, E. (2002) Neovastat (AE-941) in refractory renal cell carcinoma patients: report of a phase II trial with two dose levels. *Ann. Oncol.* **13,** 1259–1263

53. Latreille, J., Batist, G., Laberge, F., Champagne, P., Croteau, D., Falardeau, P., Levinton, C., Hariton, C., Evans, W. K., and Dupont, E. (2003) Phase I/II trial of the safety and efficacy of AE-941 (Neovastat) in the treatment of non-small-cell lung cancer. *Clin. Lung Cancer* **4,** 231–236

54. Sauder, D. N., Dekoven, J., Champagne, P., Croteau, D., and Dupont, E. (2002) Neovastat (AE-941), an inhibitor of angiogenesis: randomized phase I/II clinical trial results in patients with plaque psoriasis. *J. Am. Acad. Dermatol.* **47,** 535–541

55. Lu, C., Lee, J. J., Komaki, R., Herbst, R. S., Feng, L., Evans, W. K., Choy, H., Desjardins, P., Esparaz, B. T., Truong, M. T., Saxman, S., Kelaghan, J., Bleyer, A., and Fisch, M. J. (2010) Chemoradiotherapy with or without AE-941 in stage III non-small cell lung cancer: a randomized phase III trial. *J. Natl. Cancer Inst.* **102,** 859–865

56. Escudier, B., Choueiri, T. K., Oudard, S., Szczylik, C., Négrier, S., Ravaud, A., Chevreau, C., Venner, P., Champagne, P., Croteau, D., Dupont, E., Hariton, C., and Bukowski, R. M. (2007) Prognostic factors of metastatic renal cell carcinoma after failure of immunotherapy: new paradigm from a large phase III trial with shark cartilage extract AE-941. *J. Urol.* **178,** 1901–1905